C. R. Physique 12 (2011) 186–191

Contents lists available at ScienceDirect

Comptes Rendus Physique

www.sciencedirect.com

Propagation and plasmas: new challenges, new applications

Ionosphere scintillation effects on navigation systems

Effets de scintillations ionosphèriques sur des systèmes de navigation

Yannick Béniguel [a,*], Jean-Pierre Adam [a], Alain Bourdillon [b], P. Lassudrie-Duchesne [c]

[a] *IEEA, 13, promenade Paul-Doumer, 92400 Courbevoie, France*
[b] *IETR, University of Rennes 1, 2, rue du Thabor, 35065 Rennes cedex, France*
[c] *Telecom Bretagne, Technopôle Brest-Iroise, 29238 Brest, France*

ARTICLE INFO

Article history:
Available online 4 March 2011

Keywords:
Navigation systems
Scintillations
Positioning errors
Loss of lock

ABSTRACT

This article deals with the impact of ionospheric electron density inhomogeneities on the functionality of global navigation satellite systems emphasizing positioning errors. The scintillation characteristics of transmitted signals have been obtained using data gathered in measurement campaigns. The effects on a standard receiver are then presented. Positioning errors due to scintillations were shown to be greater than 10 meters in the worst case.

RÉSUMÉ

Cet article a pour objet l'étude de l'impact de la propagation à travers l'ionosphère, et plus particulièrement à travers les inhomogénéités à l'intérieur du milieu, sur les erreurs observées par les systèmes de navigation par satellite, en particulier pour le positionnement. Les modifications apportées sur les signaux transmis ont été évaluées à l'occasion de campagnes de mesures. L'analyse des effets sur un récepteur standard est ensuite présentée. Les erreurs de positionnement liées aux scintillations sont supérieures à la dizaine de mètres dans les pires cas.

1. Introduction

As a result of propagation through ionosphere electron density irregularities, transionospheric radio signals may experience amplitude and phase fluctuations. In equatorial regions, these signal fluctuations specially occur during equinoxes, after sunset, and last a few hours. They are more intense in periods of high solar activity. These fluctuations result in signal degradation from VHF up to C band. The corresponding errors are the most prominent errors for Global Navigation Satellite Systems (GNSS).

The signal fluctuations, referred as scintillations, are created by random fluctuations of the medium's refractive index, which are caused by inhomogeneities inside the ionosphere. These inhomogeneities such as plasma turbulences or electron density bubbles develop under several plasma instability processes. These processes start after sunset when the sun ionization drops to zero, consequently at nighttime. To produce scintillation, the irregularities sizes should be below a typical dimension (typically one km) such that the diffracting pattern is inside the first Fresnel zone. The Fresnel zone dimension

* Corresponding author.
E-mail address: beniguel@ieea.fr (Y. Béniguel).

1631-0705/$ – see front matter
doi:10.1016/j.crhy.2011.01.005

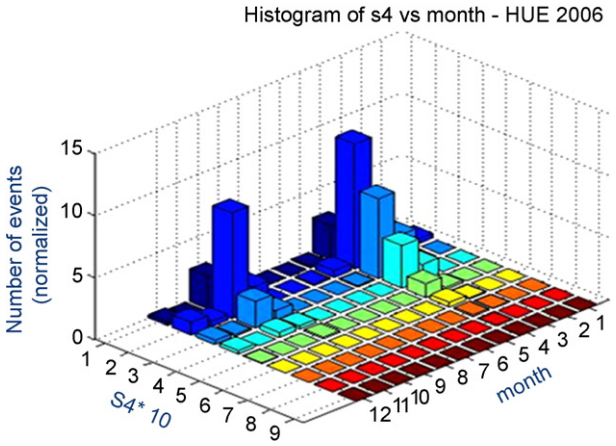

Fig. 1. Scintillation index measurement in Hué (Vietnam), year 2006.

also depends on the distance from the Ionospheric Pierce Point (usually defined at about 350 km height) to the receiver and on the frequency.

In Section 2, we present the signal scintillation characteristics, mainly the levels, the probabilities, the fades statistics and the coherence properties. These characteristics have been obtained from various measurement campaigns, in particular in South America (Doherty et al. [1], De Paula et al. [2]), India (Chandra et al. [3]) and Japan (El-Arini et al. [4] and Otsuka et al. [5]). More recently, a campaign was conducted under an ESA/ESTEC initiative (Béniguel et al. [6]) and another one is ongoing aiming to operate for the next peak of the solar cycle. A modeling activity has been conducted concurrently, also under ESA/ESTEC initiative (Béniguel [7]). The Global Ionospheric Scintillation Model (GISM) allows estimating the scintillation characteristics. It may also be used to assess the receiver performances in such an environment.

Section 3 of this article presents the effects of scintillation on a satellite navigation system receiver. It is a follow on to a previous paper on the same topic (Lassudrie-Duchesne et al. [8]) with more insight on the receiver functioning. Both the phase and intensity fluctuations have consequences on the system. In a high scintillation regime, the phase may exhibit cycle slips with consequences on the receiver phase loop. In addition, depending on the link elevation angle and as a result, on the signal to noise ratio, the scintillations may lead to loss of lock. The navigation equation is affected in all cases. Scintillation may lead to errors up to tens of meters in the worst case, making this problem a major issue for navigation systems.

2. Scintillation characteristics

For a navigation system, the parameters we are interested in, as shown in the next section, are: the probabilities of occurrence of scintillations, the scintillation indices, the fades statistics, the spectrum characteristics and the evolution of these parameters with respect to the time. The scintillation indices allow characterizing the strength of turbulence, in particular the S4 parameter which corresponds to the RMS intensity for a normalized intensity. S4 value is between 0 and 1. A value of 1 will correspond to about 35 dB peak to peak of intensity fluctuations. The time between fades and the fades duration are key parameters to assess the capability of receivers to operate in such an environment.

The Assessment of the scintillation parameters can be done either by modeling or by measurement and preferably mixing both approaches. This was done in the frame of several ESA/ESTEC contracts. A model named Global Ionospheric Scintillation Model (GISM) [7] was developed. It is continuously improved. Ionosphere scintillation measurements campaigns are still ongoing, mostly supported by ESA and EU. The results reported hereafter are taken from the PRIS measurement campaign [6]. A number of receivers were deployed both at low and high latitudes, in particular in Vietnam, Indonesia, Guiana, Cameroon, Chad and Sweden. These receivers are dedicated receivers, operating at 50 Hz, to be compatible with the scintillation spectrum as shown on Fig. 4. A data bank was constituted and the scintillation characteristics here above mentioned were derived from an extensive analysis using this data bank. Those results are used in the next section.

Fig. 1 shows measurement results obtained at Hué (Vietnam) in 2006. There is clearly a seasonal dependency with maximum at equinoxes. The peak value is on average 0.2 which is quite a low value but this is related to the fact that it corresponds to the minimum of the solar cycle.

Fig. 2 shows the correspondence between a Total Electron Content (TEC) map and a scintillation map. Those two maps were obtained by modeling using NeQuick [9] model for the TEC and GISM [7] for scintillations. They correspond to vertical links. The electron density is consequently integrated along a vertical at each grid point on the map to get the TEC. Slant observations may however exhibit higher values. The propagation length inside the ionosphere would increase in that case and by consequence the levels obtained.

Fig. 2 was obtained with a solar radio flux at 10.7 cm set to 150. It corresponds to a high value. Universal time is 10 p.m. for the TEC map and 12 p.m. for the scintillation map. At this time the peak values for the TEC occur in the Pacific Ocean

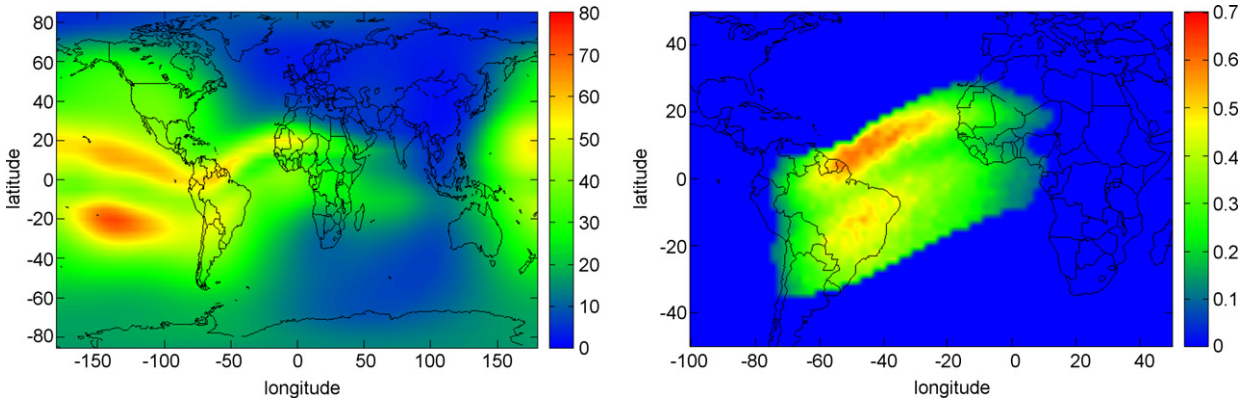

Fig. 2. TEC (left panel) and scintillation map (right panel) obtained by modeling.

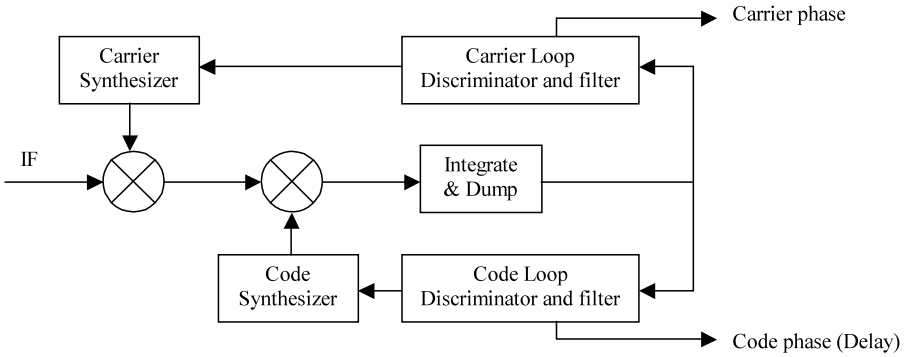

Fig. 3. Simplified GPS digital receiver channel.

area. For the scintillations the time duration of the events is a few hours after sunset. This is what gives the model. Both plots reproduce the same features regarding the peak values on both sides of the magnetic equator. The values decrease increasing the latitude. For scintillations the model calculates the effects at the equatorial regions. The high latitudes regions are also concerned by this problem but this is not taken into account by the model. The TEC maximum is 80 TEC units which is a significant value. It is directly linked to the solar flux value. The peak value for the intensity RMS (S4 parameter) is 0.7. Such a value corresponds to strong fluctuations. It is also linked to the electron density levels. Depending on the signal to noise ratio, as detailed in Section 3.3, receivers may lose lock at this level.

3. Scintillation errors

3.1. GPS receiver architecture

Any GPS receiver locking onto a GPS satellite signal has to do a two-dimensional search for the signal. The first dimension is time. The GPS signal structure for each satellite consists of a 1023 bit long pseudo-random number (PRN) sequence sent at a rate of 1.023 megabits/sec, i.e. the code repeats every millisecond. To perform acquisition in this dimension, the receiver has to set an internal clock to the correct slot among the 1023 possible time slots. This is done by trying all possible values of the time delay. Once the correct delay is found, it is tracked with a Delay Lock Loop (DLL).

The second dimension is the frequency. The receiver must correct for inaccuracies in the apparent Doppler frequency. Once the carrier frequency is evaluated, it is tracked with a Phase Lock Loop (PLL). Fig. 3 shows an extremely simplified PLL/DLL architecture. A more precise description of the GPS signal processing can be found in Ward [10].

3.2. Phase noise at receiver level

When the receiver is unable to track the carrier phase, the signal is lost. Loss of lock is directly related with PLL cycle slips. To evaluate the occurrence of cycle slips, the tracking error variance at the output of the PLL has to be considered. This variance is expressed as a sum of three terms, Conker et al. [11]:

$$\sigma_{\Phi}^2 = \sigma_{\Phi \mathrm{S}}^2 + \sigma_{\Phi \mathrm{T}}^2 + \sigma_{\Phi,\mathrm{osc}}^2 \tag{1}$$

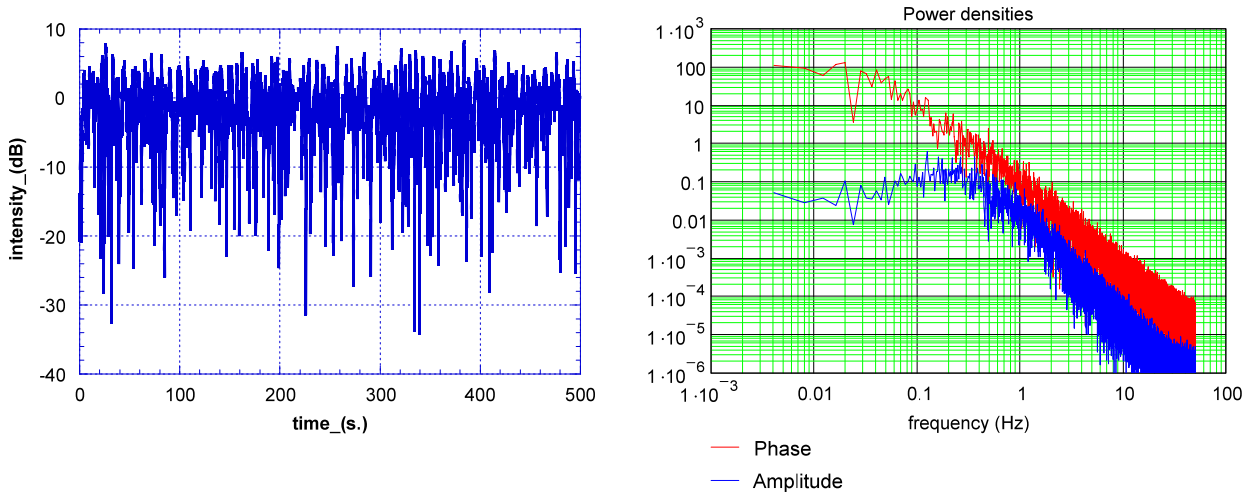

Fig. 4. Intensity time series (left panel) and corresponding spectrum (right panel).

where $\sigma_{\Phi S}$ is the phase scintillation variance, $\sigma_{\Phi T}$ is the thermal noise variance and $\sigma_{\Phi,\mathrm{osc}}$ is the receiver oscillator noise (0.122 rad) [11]. The phase variance scintillation at the output of the PLL is given by:

$$\sigma_{\Phi S}^2 = \int_{-\infty}^{\infty} \left|1 - H(f)\right|^2 S_\Phi(f)\,\mathrm{d}f \tag{2}$$

where $S_\Phi(f)$ is the Power Spectral Density of phase scintillation.

The phase scintillation spectrum is presented on Fig. 4. $|1 - H(f)|^2$ is the closed loop transfer function of the PLL and depends on k, the loop order, and f_n, the loop natural frequency. Its expression is given by (3). Typical values are $k = 3$ and $f_n = 1.91$ Hz.

$$\left|1 - H(f)\right|^2 = \frac{f^{2k}}{f^{2k} + f_n^{2k}} \tag{3}$$

When there is no scintillation, the standard thermal noise tracking error for the PLL is given by equation:

$$\sigma_{\Phi T}^2 = \frac{B_n}{(c/n_0)}\left[1 + \frac{1}{2\eta(c/n_0)}\right] \tag{4}$$

where c/n_0 is the signal to noise ratio, B_n is the receiver bandwidth, and η is the predetection time. For airborne GPS receiver, $B_n = 10$ Hz and $\eta = 10$ ms. According to Conker et al. [11], in presence of scintillation characterized by its S4 index, the variance of the thermal noise tracking error is given by:

$$\sigma_{\Phi T}^2 = \frac{B_n\left[1 + \frac{1}{2\eta(c/n_0)(1-2S_4^2)}\right]}{(c/n_0)(1 - S_4^2)} \tag{5}$$

Amplitude scintillations will increase the S4 value and consequently the thermal noise. In addition, considering the fades duration as compared to the integration time (cf. below Fig. 6), the signal to noise will drop by the fade depth.

Eq. (5) requires the evaluation of the SNR which depends on the elevation angle. Eq. (5) can be used to compute the PLL tracking error variance. Fig. 5 is a comparison of the PLL standard deviation vs c/n_0 for S4 = 0.7 and S4 = 0.5. Loss of lock is highly probable for values of the PLL standard deviation above the 15° threshold. Therefore a receiver is able to tolerate scintillation conditions if the c/n_0 is above a minimum value. This minimum is 26 dB for S4 = 0.5 and 32 dB for S4 = 0.7.

3.3. Loss of lock probability

The thermal noise appears to be the essential contribution to the PLL tracking error. It is the unique S4 dependent term in (5). The importance of the S4 index is exhibited on Fig. 5. Fig. 6 shows statistics of fade duration for different levels of S4. This fade duration always exceeds the pre-integration time.

As a consequence it corresponds to a degradation of the c/n at receiver level:

$$c/n = c/n_0 + \mathrm{Is}(\mathrm{in\,dB}) \tag{6}$$

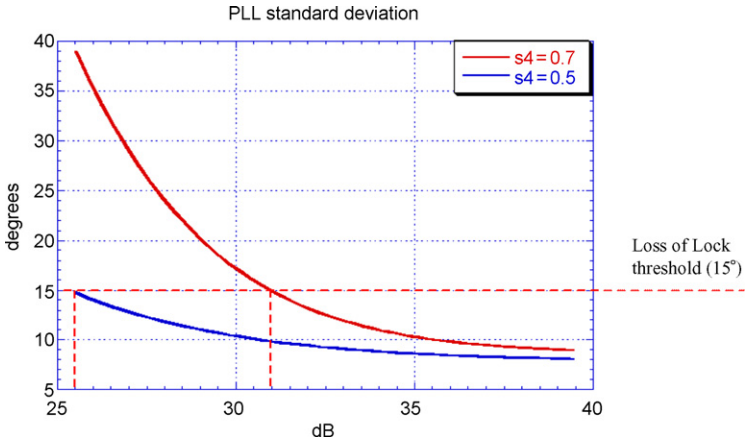

Fig. 5. PLL standard deviation vs c/n_0.

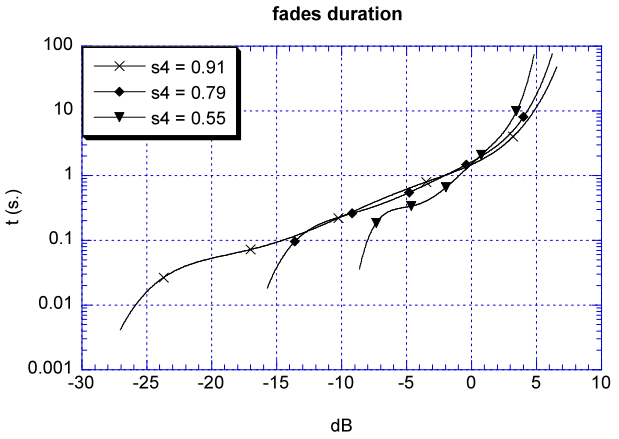

Fig. 6. Fades duration vs fade depth.

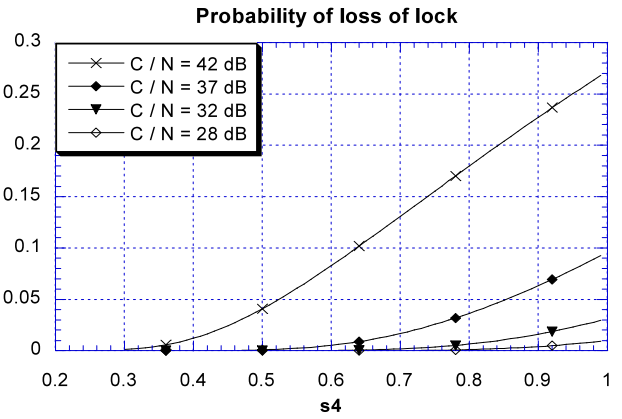

Fig. 7. Probability of loss of lock.

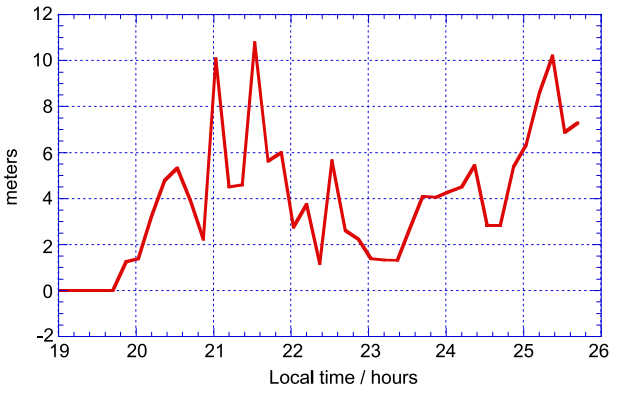

Fig. 8. Positioning error at Naha (Japan) under scintillation conditions, computed with GISM.

or, with the fractional form:

$$c/n = c/n_0 * \mathrm{Is} \tag{7}$$

where Is is the scintillation intensity. Its mean value is 1 and it has a Nakagami distribution characterized by S4. Eq. (5) is modified to take the fading into account:

$$\sigma^2_{\Phi \mathrm{T}} = \frac{B_n}{(c/n_0)\,\mathrm{Is}}\left[1 + \frac{1}{2\eta(c/n_0)\,\mathrm{Is}}\right] \tag{8}$$

This relation expresses the thermal noise as a decreasing function of the scintillation intensity. As a result, if $\sigma_{\Phi T}$ is above the 15° threshold then Is is below a value computed using (8). As the Is distribution is known for a given S4, the probability of occurrence of "Is < threshold" can be evaluated. The result is the probability of Loss of Lock. Fig. 7 presents this probability versus S4 for given values of the SNR. It can be noticed that links with high c/n_0 are quite robust. On the contrary, links with low values of c/n_0 are likely to be lost.

3.4. Positioning errors

In most cases, scintillations do not affect all visible satellites. If the number of visible satellites is above 4 then a standard receiver should be able to provide navigation information. However, the number of satellites and their positions affect the positioning precision. The Dilution Of Precision (DOP) is usually used to quantify this precision. The DOP is related to the geometrical distribution of the visible constellation. The DOP is used to derive the positioning error (σ_p) from the User Equivalent Range Error (UERE):

$$\sigma_p = \mathrm{DOP} \times \mathrm{UERE} \tag{9}$$

GISM was used to compute all scintillation parameters for each GPS satellite visible from Naha (Japan). The S4 parameter was measured for all satellites in view. The tracking error was derived from these values using formulas presented in previous sections, for typical receiver characteristics. Satellites with tracking errors above the 15° threshold were ignored for the DOP evaluation. The navigation solution was then calculated.

Even if the signal transmitted from a GPS satellite is not lost, it can be degraded enough to alter the position precision. One of the DLL functions is the measurement of the delay between the code carried by the GPS signal and the receiver internal clock. This delay is an estimation of the time needed by the GPS signal to reach the receiver. The receiver is then able to compute the satellite to receiver distance. Errors in this estimation are collected in the UERE. To take the scintillation into account, we have to consider the DLL tracking errors.

The DLL can be studied like the PLL to evaluate its tracking error variance in degrees. Satellites with high DLL tracking errors have also high PLL tracking errors and therefore they might be considered as lost and do not contribute to the UERE.

The combination of both effects is presented on Fig. 8. Satellites with PLL tracking errors above 15° were considered lost for the DOP calculation. All other links with visible satellites were used to compute a mean UERE contribution due to scintillation.

4. Conclusion

The evaluation of scintillation errors due to propagation through the ionosphere, with the two aspects of characterization of the propagation medium and modeling of the propagation impairments was presented in this paper. It was shown in particular that positioning errors may reach more than 10 meters making this error the most important for navigation systems.

The characterization of signal scintillations benefits from many measurement campaigns. The number of scintillations receivers deployed for this has significantly increased, both at low and high latitudes. This allows, in particular an improved accuracy in the modeling, a better understanding of this issue and a support to the development of mitigation techniques to minimize these errors.

References

[1] P.H. Doherty, S.H. Delay, C.E. Valladares, J. Klobuchar, Ionospheric scintillation effects in the equatorial and auroral regions, in: ION-GPS-2000, Salt Lake City, Utah, September 19–22, 2000, pp. 662–671.
[2] E. De Paula, P.H. Doherty, T. Dehel, Scintillation activity and recent measurements from the Brazilian region, in: SBAS-IONO Meeting, Maastricht, May 2001.
[3] H. Chandra, P.V.S. Ramarao, P.N. Vijay Kumar, B.M. Pathan, K.N. Iyer, A.K. Gwal, R.P. Singh, Singh Birbal, A. Dasgupta, VHF scintillations at low latitudes in India, in: Beacon Satellite Symposium, Boston College, Boston, 2007.
[4] M.B. El-Arini, R.S. Conker, S.D. Ericson, K.W. Bean, F. Niles, K. Matsunaga, K. Hoshinoo, Analysis of the effects of ionospheric scintillation on GPS L2 in Japan, in: ION-GPS-2003, Portland, OR, September 2003.
[5] Y. Otsuka, K. Shiokawa, T. Ogawa, Equatorial ionospheric scintillations and zonal irregularity drifts observed with closely-spaced GPS receivers in Indonesia, J. Meteorological Soc. Japan 84A (2006) 343–351.
[6] Y. Béniguel, J.-P. Adam, N. Jakowski, T. Noack, V. Wilken, J.-J. Valette, M. Cueto, A. Bourdillon, P. Lassudrie-Duchesne, B. Arbesser-Rastburg, Analysis of scintillation recorded during the PRIS measurement campaign, Radio Sci. 44 (2009), doi:10.1029/2008RS004090.
[7] Y. Béniguel, GIM: a global ionospheric propagation model for scintillations of transmitted signals, Radio Sci. 37 (3) (2002) 1032, doi:10.1029/2000RS002393.
[8] P. Lassudrie-Duchesne, Y. Béniguel, A. Bourdillon, R. Fleury, J.J. Valette, M. Le Huy, L. Tran Thi, Les effets de la scintillation ionosphérique sur le GPS, in: Revue de Navigation, Paris, 2010.
[9] S.M. Radicella, The NeQuick model genesis, uses and evolution, Ann. Geophys. 52 (3–4) (July–August 2009).
[10] P. Ward, Satellite signal acquisition and tracking, in: E.D. Kaplan (Ed.), Understanding GPS Principles and Applications, Artech House, Boston, 1996, pp. 119–208.
[11] R.S. Conker, M.B. El-Arini, C.J. Hegarty, T. Hsiao, Modeling the effects of ionospheric scintillation on GPS/SBAS availability, Radio Sci. 38 (1) (2003), doi:10.1029/2000RS002604.